



ISSN: 0067-2904

Determination of Differential Cross-Section of $(n+^{89}\text{Y})$ Elastic and Inelastic Scattering using Eikonal Approximation

Akram Mohammed Ali*, Hajer Mezban Mohammed

Department of Physics, College of Science, University of Anbar, Anbar, Iraq

Received: 27/4/2021

Accepted: 28/8/2021

Published: 30/6/2022

Abstract

Neutron differential-elastic and inelastic scattering cross-sections of Yttrium-89 isotope were calculated at energies 8,10,12,14, and 17 MeV, at angles distributed between 20° and 180° in the center of mass frame. The obtained results data were interpreted using a spherical optical potential model and Eikonal approximation, to examine the effect of the first-order Eikonal correction on the effective potential. The real and imaginary parts of optical potential were calculated. It was found that the nominal imaginary potential increase monotonically while the effective imaginary one has a pronounced minimum around $r = 6\text{fm}$ and then increases. The analysis of the relative energy of the projectile and reaction product was taken into account. The main results were compared with available experimental data at EXFOR.

Keywords: Optical potential, Eikonal approximation, differential scattering cross-sections, gamma distribution, yttrium-89.

تحديد المقطع العرضي التفاضلي لتفاعل $(n+^{89}\text{Y})$ للثشت المرن وغير المرن باستخدام تقريب إيكونال

اكريم محمد علي* ، هاجر مزبان محمد

قسم الفيزياء ، كلية العلوم ، جامعة الأنبار ، العراق ، العراق.

الخلاصة

تم حساب المقاطع العرضية التفاضلية للثشت المرن وغير المرن لتفاعل النيوترون مع نظير الإيتريوم 89 عند الطاقات 8, 10, 12, 14 و 17 ميغا إلكترون فولت ، وعند الزوايا الموزعة بين 20° و 180° في إطار مركز الكتلة. تم تفسير بيانات النتائج التي تم الحصول عليها باستخدام نموذج الجهد البصري الكروي وتقريب إيكونال لدراسة تأثير التصحيح تقريب إيكونال من الدرجة الأولى على الإمكانيات الفعالة ، قمنا بحساب الأجزاء الحقيقية والخيالية للجهد البصري ووجدنا أن الجهود البصرية التخيلية الاسمية تزداد بشكل رتيب بينما الاحتمال التخيلي الفعال. تم أخذ تحليل الطاقة النسبية للمنتج المقذوف ومنتج التفاعل في الاعتبار. تمت مقارنة النتائج مع البيانات التجريبية المتاحة في موقع EXFOR.

*Email: dr.akram@uoanbar.edu.iq

1. Introduction

The study of nuclear properties has attracted wide attention from many researchers to understand the nuclear structure. To fulfill this, besides the nuclear reaction of many nuclei, the cross-section of the differential elastic and inelastic scattering of the neutron interacting with these nuclei are used. Many studies have been done for this purpose, where the neutron differential-elastic-scattering cross-sections range from 4 to 10 MeV, with energy intervals of around 500 keV, and 20 or more angles ranging from 20° to 160° [1]. Neutron differential-elastic-scattering cross-sections of bismuth were measured at 0.5 MeV with intervals ranging from 4.5 to 10.0 MeV[1].

Proton reaction scattering cross-section is studied with wide high incident energy region using on eikonal approximation. These high energies give a small scattering angle that depends on the nucleon-nucleus optical potential. The proton-carbon optical potential is calculated using a folding integral of the nucleon-nucleon transition amplitude and matter density of carbon. Analytical formulas of optical potential are used to present in position-space representation for carbon isotope by using harmonic well nuclear densities ($A < 20$) [2]. The cross-sections of nucleus-nucleus scattering were also obtained at 600 MeV using double-folding optical model potentials based on effective nucleon-nucleon (NN) interaction and folding potential (tpp) approximation [3].

^{9,10,11,12}Be isotopes were tested upon proton projectile to have elastic scattering at a wide energy range from 3 to 200 MeV/nucleon using the optical model with the partial-wave expansion method. For higher energies, the Eikonal approximation is successfully used. The volume integrals of the optical potential (OP) parts have systematic energy dependencies and can be parameterized as functions of energy. From these parametrizations, an energy-dependent optical potential (OP) can be obtained[1, 4].

Yttrium-89 is a natural isotope near the ⁹⁰Zr isotope magic proton number; it has an abundance of 100%. Therefore, the nuclear data of this isotope need to be investigated and to study how it is affected by neutrons as it is used in fast reactors and fusion reactors. So, present the microscopic analysis of the data of an elastic and inelastic neutron scattering using yttrium isotope(Y-89) over a range of energies (8-17) MeV / nucleon. This paper describes the analysis of the standard optical model of this target. For input parameters, the parameter input reference (RIPL-3 library) was used. This data was used in both the real and imaginary parts of the potential visual model, with particular emphasis, in this study, on the theoretical dependence of the optical model's capabilities.

The neutron differential cross-sections of the elastic scattering were calculated using Eikonal approximation for many-body scattering which is based on Glauber's theory and were compared with experimental data obtained from the EXFOR library. Besides the calculation of differential cross sections of inelastic scattering, these results were compared with each other at different energies. The theoretical aspects are given in section 2, the calculation results are shown in section 3, and concluding remarks are shown in section 4.

2. Theoretical aspects:

The current problem involves a neutron with energy E colliding with a target with mass number A and is scattered by a microscopic spherical optical potential U_{opt} , which can be expressed as[5]:

$$U_{opt} = -V_o f(r, R_r, a_r) - iW_o f(r, R_i, a_i) \quad (1)$$

where: $f(r, R, a) = [1 + \exp(\frac{r-R}{a})]^{-1}$

the radii of the colliding system are:

$$R_{r(i)} = r_o (A_p^{1/3} + A_t^{1/3}) \quad (2)$$

where V_o , W_o , $R_{r(i)}$ and $a_{r(i)}$ are the real and imaginary part of the potential, real and imaginary radii parameters in *fm*, and real and imaginary diffuseness parameters in *fm*. A_p and A_t are the projectile and target mass numbers, respectively.

When de Broglie's wavelength of the incident particle $\lambda = h/p$ is sufficiently short compared to the distance over which the potential varies appreciably, the Eikonal approximation is very helpful in the study of scattering.

Using the Eikonal approximation for wave functions [6]:

$$\Psi^{(-)*}(r)\Psi^{(+)}(r) \approx \exp\{iq \cdot r + i\chi(b)\} \quad (3)$$

Where: $\chi(b)$ denotes the Eikonal phase, which is given by:

$$\chi(b) = -\frac{1}{\hbar v} \int_{-\infty}^{\infty} dz U_{opt}(r) \quad (4)$$

where v is the projectile relative velocity in the z -direction. The validity conditions of the Eikonal approximation are: (a) forward scattering, i.e., $\theta \ll 1$ radian, and (b) small energy transfers from the bombarding energy to the projectile's or target's internal degrees of freedom. At $E_{lab} \geq 50$ MeV/nucleon, both conditions are perfectly applicable to direct processes in nuclear scattering [7].

The equations for calculating elastic scattering amplitudes with Eikonal wavefunctions are given by [7]:

$$f_{E=\frac{k}{i}} = \int_0^{\infty} b db J_0(qb) [\exp\{i\chi(b)\} - 1] \quad (5)$$

The momentum transfer, $q = 2k \sin(\theta/2)$, is expressed by incident projectile momentum k and θ , the scattering angle. The impact parameter is $b = (l + 1/2)/k$. The absolute square of the scattering amplitude is used to calculate the elastic differential cross-section [7]:

$$\frac{d\sigma}{d\Omega} = |f(\theta)|^2 \quad (6)$$

The total elastic cross-section is obtained by integrating over the solid angle [7]:

$$\sigma_{el.}^t = \frac{d\sigma}{d\Omega} d\Omega$$

$$\sigma_{el.}^t = 4\pi \int_0^{\infty} [1 - e^{-\text{Im} \chi} \cos(\text{Re} \chi)] b db - 2\pi \int_0^{\infty} [1 - e^{-2 \text{Im} \chi}] b db \quad (7)$$

where total nuclear inelastic cross-section using optical potential is obtained by [2]:

$$\sigma_{inel.}^t = 2\pi \int_0^{\infty} [1 - e^{-2 \text{Im} \chi}] b db \quad (8)$$

The scattering amplitude satisfies the optical theorem, so the total cross-section is obtained by [2]:

$$\sigma_{tot} = \sigma_{el.}^t + \sigma_{inel.}^t$$

$$\sigma_{tot} = \frac{4\pi}{k} \text{Im} f(\theta = 0) = 4\pi \int_0^{\infty} [1 - e^{-\text{Im} \chi} \cos(\text{Re} \chi)] b db \quad (9)$$

3. Results and discussion

The differential cross-sections of $n + {}^{89}\text{Y}$ elastic and inelastic scattering are calculated using DWEIKO code [7] where a limited number of parameters are included for the falling neutron's spherical potential. For the ${}^{89}\text{Y}$ nuclei, the neutron potential energy depends on the isotope of yttrium ($Z = 39$, $A = 89$) and is 8,10,12,14, and 17 MeV. Which were taken into account in the current calculations to cover the same energy range for the same target charge and mass. The Visual File Coordinated Search Project (RIPL-3) contains parameters for Optical Model Capabilities (OMP). For each incident energy, Table 1 lists the optical model potential parameters used in this study for the ${}^{89}\text{Y}$ target. The real part, V , is responsible for the elastic scattering that describes the normal nuclear interaction between the target and the shell and thus can resemble the shell model's potential. The imaginary part, W , is responsible for the absorption [8]. The global potential parameters in RIPL-3 are valid for the nuclear several radial distances (r) as well as the real and imaginary potentials strengths V_o and W_o are but in this calculation, they have varied them and r and a were kept fixed as in Table 1.

The main results of the excited nuclei are $\langle r^2 \rangle = 18.788$ [9] with root mean square $\langle r^2 \rangle^{1/2} = 4.334$ [10] for energies 8,10,12,14 and 17 MeV, respectively. Lorentz factor (1.009,1.011,1.013,1.015,1.018) wavenumber (k)=0.613,0.686,0.752,0.812,0.896 and eta η (Sommerfeld parameter) for all energies is zero because the charge of projectile (neutron) is zero and number of coupled channels for all energies is (9). Total nuclear reactions cross section = -8944.31, -6979.35, -4857.22 mb for 12,14 and 17 MeV, respectively. The excitation cross-sections for nucleus from state to state are tabulated in Table 2.

Table 1- Parameters for optical potential used for calculating the scattering angular distribution from RIPL-3.

E_{in} MeV	V_v MeV	r_v fm	a_v fm	W_v MeV	r_{wv} fm	a_{wv} fm	W_s MeV	r_{ws} fm	a_s fm	V_{so} MeV	r_{so} fm	a_{so} fm
8	48.4	1.22	0.67	0.6	1.22	0.67	5.5	1.27	0.53	5.8	1.05	0.56
10	47.7	1.22	0.67	0.8	1.22	0.67	5.7	1.27	0.53	5.7	1.05	0.56
12	47	1.22	0.67	0.9	1.22	0.67	5.8	1.27	0.53	5.7	1.05	0.56
14	46.3	1.22	0.67	1.1	1.22	0.67	5.9	1.27	0.53	5.7	1.05	0.56
17	45.3	1.22	0.67	1.3	1.22	0.67	5.8	1.27	0.53	5.6	1.05	0.56

Table 2- Excitation cross section in (mb) for neutrons with energies 8,10,12,14 and 17 MeV.

Energy	8 MeV	10 MeV	12 MeV	14 MeV	17 MeV
State 2	0.425E+04	0.292E+04	0.235E+04	0.196E+04	0.161E+04
State 3	0.147E+02	0.117E+02	0.987E+01	0.813E+01	0.609E+01
Total	0.426E+04	0.293E+04	0.236E+04	0.197E+04	0.161E+04

The calculation of differential cross-section for elastic $n+^{89}\text{Y}$ scattering at some energies in the frame of center of mass (CM) is represented in Figure 1 compared with observed differential elastic cross-sections. The solid line represents the calculated differential cross-section while the black dots represent the experimental data. From Figure 1, it can be noted that the Eikonal model for the neutron leads to better dependence on the angle both for the calculated and the experimental data. The cross-section of the experimental data has a significant flexure for each energy at a different angle. The reason for this is that the experimental data include the uncertainties of measurement that were not included in the theoretical calculations. The Eikonal model results predict a higher cross-section for smaller angles and a much falloff with larger angles.

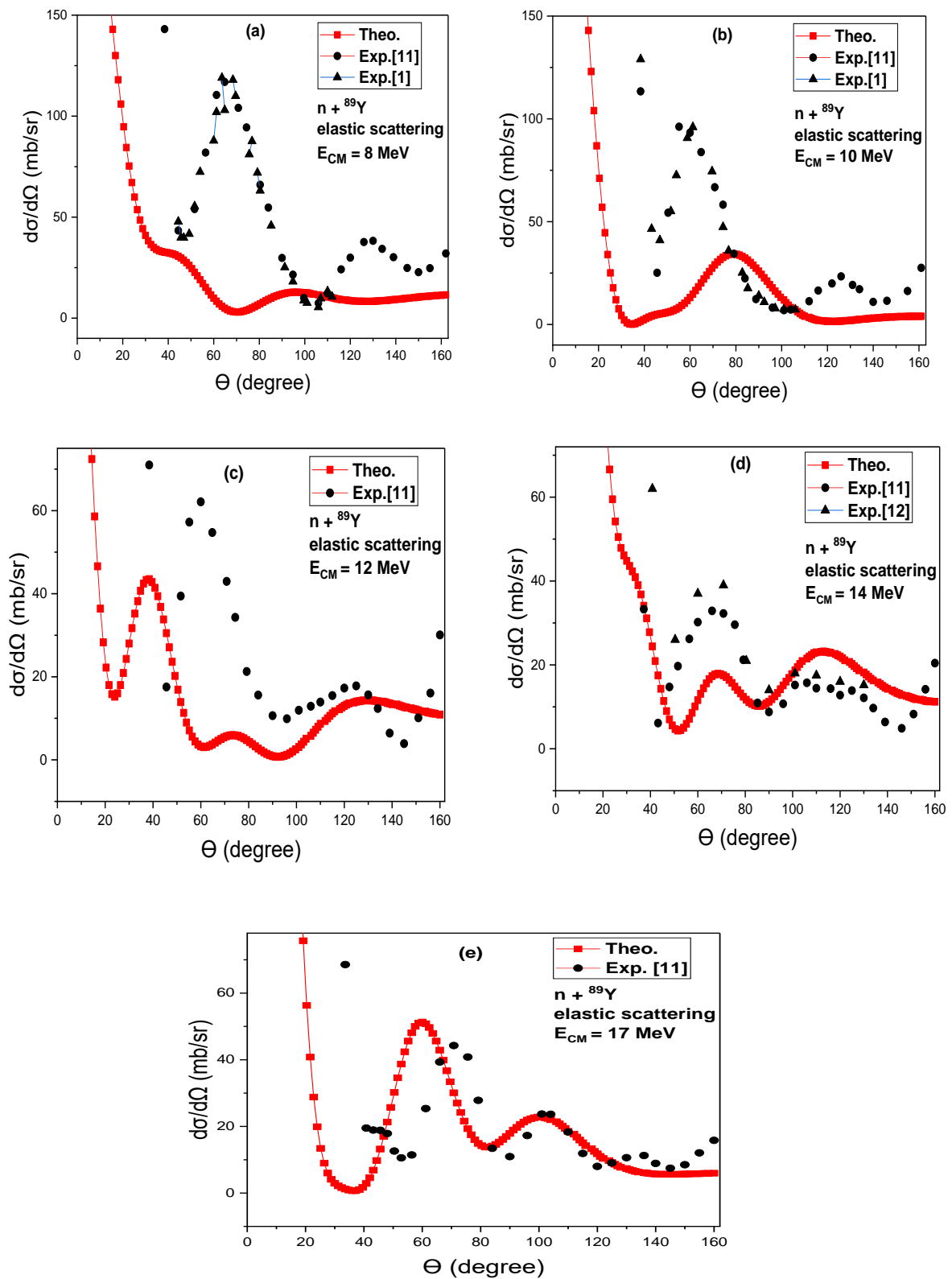


Figure 1- ($n + {}^{89}\text{Y}$) interaction elastic differential cross section. The calculation performed at different energies (a)8, (b)10, (c)12, (d)14 and (e)17 MeV calculated in the center of mass frame compared with the experimental data [1, 11, 12] .

By assuming the projectile to be spherical (neutron) and a deformed target (^{89}Y), the analysis of the inelastic differential cross-section has been done by taking the coupled channels between two states of the target. The deformation parameter (β_λ) are ($\beta_2, \beta_3 = 0.425, 0.736 \text{ fm}$) corresponding to the states of excitation energies of low lying vibrational states 2^+ and 3^+ ($E_2, E_3 = 10.9, 13.5 \text{ MeV}$) comparing with experimental one for $E_2 = 11.9 \text{ MeV}$ [9]. Calculations were done in two frames, CM and lab., for different neutron incident energies, Figure 2. It is concluded that the behavior of the two frames is the same with few differences.

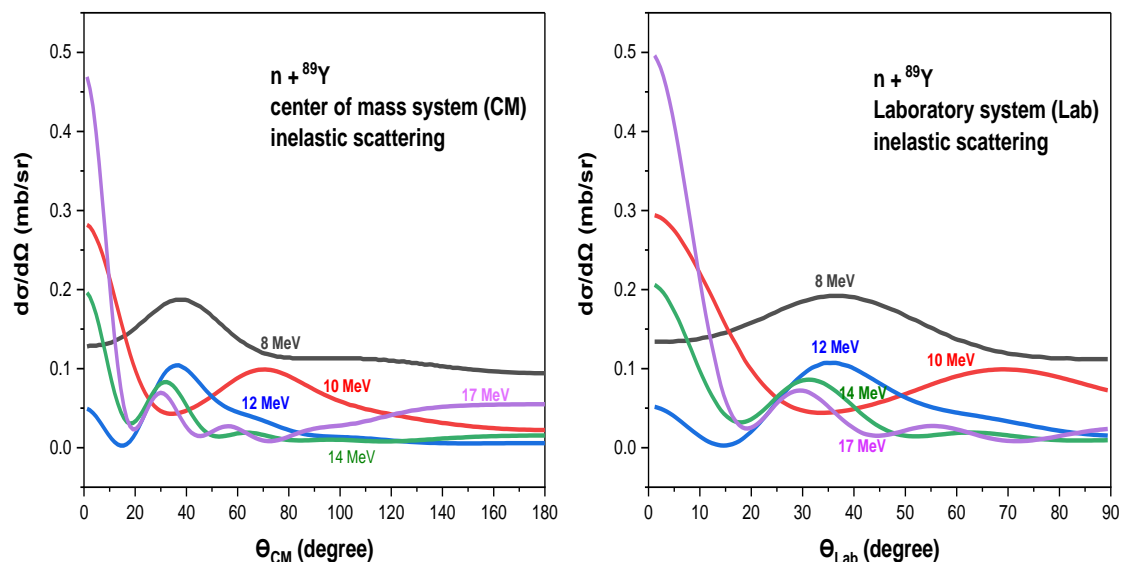


Figure 2-The center of mass and laboratory systems differential inelastic cross-section at different energies (8,10,12,14, and 17) M eV.

To examine the effect of the first-order Eikonal correction on the effective potential, Both the real and the imaginary parts of an effective potential were plotted, as shown in Figure 3. In this figure, the colored solid curves denote the effective potential $U_{eff}(r)$. As this Figure shows, there is a dramatic difference between the two potentials, especially in the small r regions. The drastic changes in the effective potential are due to the correction terms containing the product of the real and the imaginary potentials and their derivatives. The degree of change is noticed more in the imaginary potential than in the real one. As Figure 3(b) shows, the nominal real potential increases monotonically while the effective imaginary one has a pronounced minimum around $r = 6\text{fm}$ and then increases. However, the discrepancy in the r regions (1-5) fm is not important because the surface region of the colliding nuclei contributes in high values to the differential cross-section.

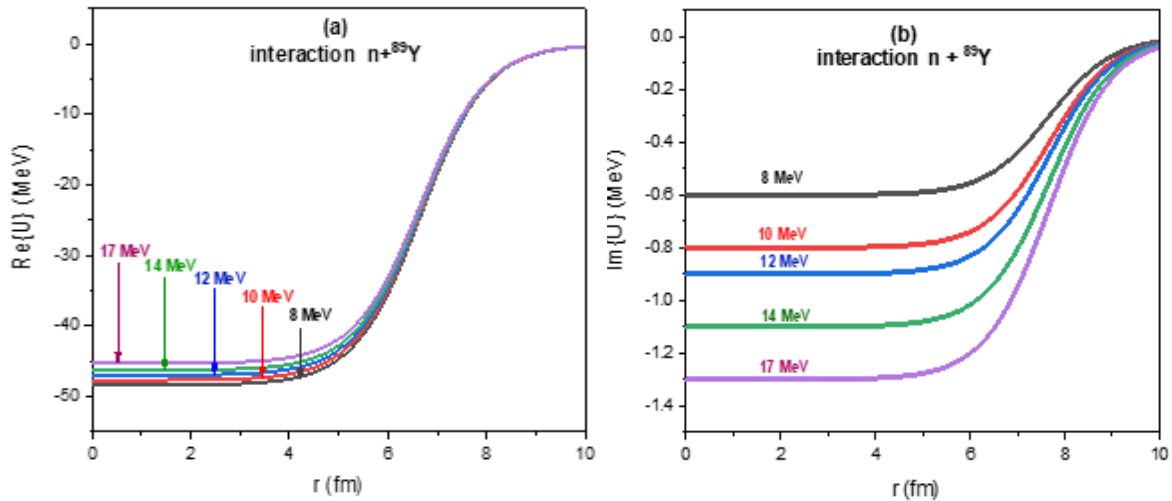


Figure3-Real and imaginary optical potentials used in the optical model analysis for different energies (MeV) for elastic scattering.

After the nucleus collides and is excited it decays from final state 2^+ to the initial 0^+ state by gamma emission. Gamma-ray transition coefficients were calculated by gamma strength function W that depended on θ_{CM} of the neutron, multipolarity of gamma-ray, and spin-parity of the final and initial states as well as the resulting angular momentum produced from the reaction. This function is given as[10]:

$$W(\theta) = A_0[1 + A_2P_2(\cos\theta) + A_4P_4(\cos\theta)]$$

Where: P_n is Legendre polynomials and A_n are expansion coefficients of polynomials. The Lorentz factor β of the projectile velocity motion in the frame of center of mass is (1.013) used to find pure transitions of $E1=2^+ \rightarrow 0^+$ (10.9 MeV) and $E2=3^+ \rightarrow 0^+$ (13.5MeV) radiations as (0.8649 and 0.5898 $e^2.b$). The contour plot of the potential energy surfaces presented in Figure 4 shows that for neutron angle there are different angular distributions for θ ranging from (0°) to (180°) with (1°) step. The different values of γ - ray angular distribution $W(\theta)$ found it is varied between 20° and 180° for $n + ^{89}\text{Y}$. Also, Figure 4 shows the same previous relation between the deformation type of the target as prolate and oblate

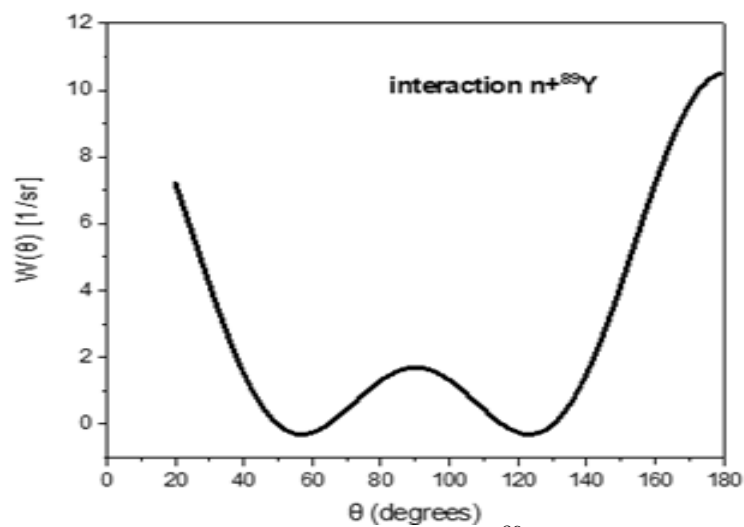


Figure 4-Gamma-ray angular distribution of exposing ^{89}Y nuclei to 14MeV neutron energy calculated in CM frame.

To have a complete description of the $n+^{89}\text{Y}$ reaction, the analysis of the relative energy of the projectile and reaction products must be involved. Figure 5 shows the summary of the total reaction cross-section as a function of the energy of the incident neutron. At low energy the nuclear reaction occurs in two scales of reactions, the direct reaction takes time as the neutron pass by the target nuclei. This component of reaction contributes very smoothly to the cross-section with energy. The second component is the compound nuclear state of ^{89}Y nuclei that contribute to total cross-section fluctuating rapidly to nearly 7 MeV then as energy increases, compound nucleus state density be large as it involves many states.

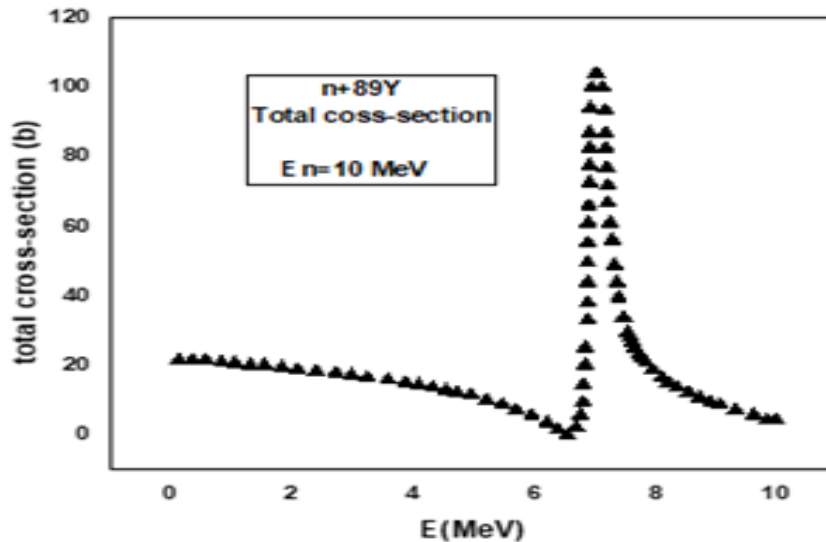


Figure 5- Total cross-section for $n+^{89}\text{Y}$ reaction at incident neutron energy close to 10 MeV.

4. Concluding Remarks:

Differential cross-section of $n+^{89}\text{Y}$ scattering predicted using optical potential was considered in different energies and made computations over the nuclear matter densities of ^{89}Y and (NN) transition amplitude. A comparison with available experimental data for target nuclei was made. Our findings could be useful in studying the elastic scattering of a many-body system. A more detailed description of our work will include a comparison with elastic scattering data from the laboratory frame.

5. Conflict of Interest

Conflict of Interest: The authors declare that they have no conflicts of interest.”

References:

- [1] R. Lawson, P. Guenther, and A. Smith, "Search for the Fermi-surface anomaly in fast-neutron scattering from yttrium," *Physical Review C*, vol. 34, p. 1599, 1986.
- [2] M. M. Chit, T. Wint, K. M. Win, and K. M. Maung, " Analysis of proton scattering from carbon isotopes," *J. Myanmar Academy of Arts and Science*, vol. XVIII, no. 2B, pp. 73-84, 2020.
- [3] M. E.-A. Farid, K. O. Behairy, Z. M. M. Mahmoud, and K. O. Hussein, "Analysis of ^6Li Scattering at 600 MeV," *Brazilian Journal of Physics*, vol. 44, pp. 73-90, 2014.
- [4] H.M. Maridi, M. Y. H. Farag, and E. H. Esmael, "Analysis of proton scattering of stable and exotic light nuclei using an energy-dependent microscopic optical potential," *EPJ Web of Conferences*, vol. 107, article no. 08007, 2016.
- [5] R. R. Roy and B. P. Nigam, *Nuclear physics: theory and experiment*: Wiley, 1967.
- [6] R. J. Glauber and G. Matthiae, "High-energy scattering of protons by nuclei," *Nuclear Physics B*, vol. 21, no.2, pp. 135-157, 1970.

- [7] C. A. Bertulani, C. M. Campbell, and T. Glasmacher, "A computer program for nuclear scattering at intermediate and high energies," *Computer physics communications*, vol. 152, no. 3, pp. 317-340, 2003.
- [8] I. T. Al-Alawy and R. I. Ali, "Optical model potential using CINDA library for neutron-induced cross section reactions for spherical uranium-235,238 isotopes," *International Letters of Chemistry, Physics and Astronomy*, vol. 60, pp. 66-73, 2015.
- [9] A. Mukherjee, M. Dasgupta, D. J. Hinde, K. Hagino, J. R. Leigh, J. C. Mein, C. R. Morton, J. O. Newton, and H. Timmers, "Dominance of collective over proton transfer couplings in the fusion of ^{32}S and ^{34}S with ^{89}Y ," *Physical Review C*, vol. 66, p. 034607, 2002.
- [10] N. Cieplicka, B. Fornal, K. Maier, B. Szpak, R. Broda, W. Królas, *et al.*, "Angular distributions of γ -rays from ^{210}Bi produced in $^{208}\text{Pb} + ^{208}\text{Pb}$ deep-inelastic reactions," *Acta Physica Polonica Series B*, vol. 45, no. 2, pp. 205-210, 2014.
- [11] G. M. Honoré, R. S. Pedroni, C. R. Howell, H. G. Pfützner, R. C. Byrd, G. Tungate, and R. L. Walter, "Differential cross sections and analyzing powers for neutron elastic scattering from Y 89 between 8 and 17 MeV," *Physical Review C*, vol. 34, p. 825, 1986.
- [12] B. E. Leshchenko, M. E. Gurtovoj, A. S. Kukhlenko, and V. I. Strizhak, "Excitation of collective states of some medium nuclei by 14 MeV neutrons," *Yadern. Fiz.*, vol. 15, no. 1, pp. 10-17, 1972.